EPJ Web of Conferences **83**, 02015 (2015)
DOI: 10.1051/epjconf/20158302015

A generalized mean-squared displacement from inelastic fixed window scans of incoherent neutron scattering as a model-free indicator of anomalous diffusion confinement

Felix Roosen-Runge[a] and Tilo Seydel

Institut Laue-Langevin, 71 avenue des Martyrs, 38042 Grenoble, France

Abstract. Elastic fixed window scans of incoherent neutron scattering are an established and frequently employed method to study dynamical changes, usually over a broad temperature range or during a process such as a conformational change in the sample. In particular, the apparent mean-squared displacement can be extracted via a model-free analysis based on a solid physical interpretation as an effective amplitude of molecular motions. Here, we provide a new account of elastic and inelastic fixed window scans, defining a generalized mean-squared displacement for all fixed energy transfers. We show that this generalized mean-squared displacement in principle contains all information on the real mean-square displacement accessible in the instrumental time window. The derived formula provides a clear understanding of the effects of instrumental resolution on the apparent mean-squared displacement. Finally, we show that the generalized mean-square displacement can be used as a model-free indicator on confinement effects within the instrumental time window.

1. Introduction

The apparent mean-squared displacement (MSD) $\langle u^2_{\mathrm{app}}\rangle$ determined from elastic fixed window scans of incoherent neutron scattering have been used to explore dynamical changes as a function of parameters such as temperature, pressure, external fields or reaction time. Well-known examples include the dynamics in glass-forming systems [1–3] and bioprotectant disaccharides [4] as well as the protein dynamical transition [5,6], in particular the coupling of protein dynamics to the environment [7–10].

The apparent MSD combines several relevant features. First, the apparent MSD exploit the general strength of incoherent neutron scattering to explore self-dynamics in confined geometries on molecular length scales. Second, in practice, it allows a model-free analysis of the scattering intensity at zero energy transfer, where also the scattering intensity is maximal. Third, in interpretation, a physical picture of the dynamical changes is obtained by considering the apparent MSD as an effective amplitude of motion, which allows relative comparison between different systems as well as connections to simulational studies.

In the last decade, the physical meaning of the apparent MSD has been explored in several studies on the dependence on the instrumental resolution, from both theoretical [11–16] and experimental view points [17]. In a different approach to advance the analysis, the apparent MSD has been explicitly calculated using a dynamical model for the full quasi-elastic spectra, thereby allowing to separate internal from global dynamics during protein denaturation [18,19].

Recent instrumental developments, in particular at the IN16B (ILL), opened new opportunities for inelastic fixed window scans, i.e. scans of the incoherent scattering intensity at fixed finite energy transfer [20–23]. In this context, it is interesting whether the concept of the apparent MSD can be extended to inelastic scans to provide model-free analysis and interpretation. In this paper, we introduce a generalized MSD $\langle u^2\rangle_\omega$ and derive a direct connection of $\langle u^2\rangle_\omega$ to the real physical time-dependent MSD accessible within the instrumental time window. We explicitly evaluate $\langle u^2\rangle_\omega$ for generic types of motions and discuss the physical meaning as well as limitations and opportunities for a model-free analysis. In particular, we suggest $\langle u^2\rangle_\omega$ as a model-free indicator for the strength of confinement effects within the instrumental time window.

2. The generalized mean-squared displacement $\langle u^2\rangle_\omega$

For a fixed energy transfer ω, the experimental intensities given from the van-Hove scattering law $S(q,\omega)$ convoluted by the experimental resolution function $\hat{R}(\omega)$ can be expanded as a series in q around $q=0$ [14]:

$$S_{\mathrm{exp}}(q,\omega) = S(q,\omega)\otimes\hat{R}(\omega) \tag{1}$$

$$= \frac{1}{\sqrt{2\pi}}\int_{-\infty}^{\infty} dt\, e^{-i\omega t}\left\langle \sum_j \exp[-iq\Delta r_j(t)]\right\rangle R(t) \tag{2}$$

$$= \hat{R}(\omega) - \frac{q^2}{2}\frac{1}{\sqrt{2\pi}}\int_{-\infty}^{\infty} dt\, e^{-i\omega t}\langle\Delta r^2\rangle(t)R(t) + \frac{q^4}{24}\frac{1}{\sqrt{2\pi}}\int_{-\infty}^{\infty} dt\, e^{-i\omega t}\langle\Delta r^4\rangle(t)R(t) + \mathcal{O}(q^6). \tag{3}$$

[a] e-mail: roosen-runge@ill.eu

Here, $\langle \Delta r^2 \rangle = \langle \sum_j \Delta r_j(t)^2 \rangle$ corresponds to the real time-dependent MSD, summed over the full sample with all atoms j. The instrumental time window and, in particular, the restricted temporal coherence of the neutron beam are accounted for by the resolution function $R(t)$.

Inspired by the dynamic Debye-Waller factor $\exp\left(-\langle u^2_{\rm vib}\rangle q^2/3\right)$, the second term in Eq. (3) can be used to define the generalized MSD,

$$\langle u^2 \rangle_\omega = -\lim_{q\to 0} \frac{3}{q^2} \log\left[S_{\rm exp}(q,\omega) \Big/ \hat{R}(\omega) \right] \qquad (4)$$

$$= \frac{3}{2} \frac{1}{\sqrt{2\pi}} \int_{-\infty}^{\infty} dt\, e^{-i\omega t} \langle \Delta r^2 \rangle(t) R(t) \Big/ \hat{R}(\omega), \qquad (5)$$

which thus corresponds to a Fourier transform of the real time-dependent MSD truncated by the instrumental resolution function.

We remark that the neglection of higher order terms in the limit of zero q is the analogue to the well-known Gaussian approximation that has been applied frequently to extract the apparent MSD. Using the series approximation, we introduce a very general account that can also easily be compared to earlier results on non-Gaussian behavior, generally causing deviations in the q^4 term [11]. In experiments, the limit of zero q cannot be reached, and a polynomial fit in q^2 up to order q^4 should be used to obtain $\langle u^2 \rangle_\omega$ [18]. In this case, $\langle u^2 \rangle_\omega$ can be reliably obtained as long as the q^4 term is smaller than the q^2 term at the minimum value $q_{\rm min}$:

$$\frac{q^2_{\rm min}}{12} \int_{-\infty}^{\infty} dt\, e^{-i\omega t} \langle \Delta r^4 \rangle(t) R(t) < \int_{-\infty}^{\infty} dt\, e^{-i\omega t} \langle \Delta r^2 \rangle(t) R(t). \qquad (6)$$

Although an exact estimation thus depends on the underlying stochastic process, a simple diffusive displacement with $\langle \Delta r^4 \rangle = 3\langle \Delta r^2 \rangle^2$ can be used for an estimation of the maximum MSD that would allow a reliable extraction:

$$\langle \Delta r^2 \rangle_{\rm max} = \max_{t<t_{\rm max}} \langle \Delta r^2 \rangle(t) < 4\, q^{-2}_{\rm min}. \qquad (7)$$

Here, $t_{\rm max}$ represents the maximum coherence time, i.e. the largest t with non-negligible value of $R(t)$.

2.1. Explicit evaluation of $\langle u^2 \rangle_\omega$

Since analytical evaluation requires an explicit form of the resolution function $\hat{R}(\omega)$, we choose a Gaussian resolution function as found e.g. in the neutron backscattering spectrometer IN16B at the ILL:

$$\hat{R}(\omega) = \frac{1}{\sqrt{2\pi}\,\Delta\omega} \exp\left(-\frac{\omega^2}{2\Delta\omega^2}\right) = \frac{1}{\sqrt{2\pi}} \int_{-\infty}^{\infty} dt\, e^{-i\omega t} R(t)$$
$$\text{with} \quad R(t) = \frac{1}{\sqrt{2\pi}} \exp\left(-\frac{\Delta\omega^2 t^2}{2}\right). \qquad (8)$$

The outlined method can be easily extended to symmetric resolution functions that can be approximated by a sum of Gaussian profiles centered around zero energy transfer.

Table 1 summarizes several real MSD $\langle \Delta r^2 \rangle(t)$ and the resulting generalized MSD $\langle u^2 \rangle_\omega$. Besides very fast motions beyond the instrumental time scale, free diffusion, free ballistic motion and super- and subdiffusive motions, also two tentative generic forms for the real time-dependent MSD are evaluated. These forms combine $\langle \Delta r^2 \rangle(0) = 0$ with two limiting behaviors relative to the time scale $\tau_{\rm conf} = 1/\lambda$ on which confinement effects set in (see Table 1, last two rows). For small times $t \ll \tau_{\rm conf}$, free diffusive or ballistic motion is found, respectively. At long times, the confinement of the experimental system is accounted for by the constant value of $\langle \Delta r^2 \rangle(t \gg \tau_{\rm conf}) = \sigma^2 = {\rm const}$. The generic forms correspond to averaged versions of the general form $\langle \Delta r^2 \rangle(t) = \sum_j \sigma_j^2 (1 - C_j(t))$ with the atom-specific amplitude σ_j^2 and the stationary position relaxation function $C_\alpha(t)$ [24]. We remark that for these generic forms, the relaxation constant λ corresponds to a relaxation with respect to confinement effects, and not the relaxation constant of free motions.

Some exemplary results of $\langle u^2 \rangle_\omega$ for a tentative generic model of diffusive motion in confinement with $\langle \Delta r^2 \rangle(t) = \sigma^2[1 - \exp(-\lambda|t|)]$ are shown in Fig. 1. For simplicity of notation and in order to represent the results in resolution-independent quantities, we use the dimensionless units $\Omega = \omega/(\sqrt{2}\Delta\omega)$ and $\Lambda = \lambda/(\sqrt{2}\Delta\omega)$.

For all evaluated examples, $\langle u^2 \rangle_\omega$ decreases strongly with the energy transfer Ω. Note that this general behavior is caused by the generic shape of any real MSD and not by specific features of these examples: The initial increase of the real MSD $\langle \Delta r^2 \rangle(t)$ starting from $\langle \Delta r^2 \rangle(0) = 0$ is reflected in negative Fourier components at high Ω.

Since experiments and simulations only provide a finite range of energy transfers, the large negative values for large Ω render a direct back-transform from $\langle u^2 \rangle_\omega$ to $\langle \Delta r^2 \rangle(t) R(t)$ very inaccurate, if not impossible. Furthermore, also regularized fitting methods result in severely ill-conditioned procedures, since $\langle u^2 \rangle_\omega$ for different Λ and different models appears very much alike, if only a finite number of ω_i is measured. Thus, no general model-free method can be used to extract information on the accessible MSD $\langle \Delta r^2 \rangle(t) R(t)$.

2.2. Dependence of $\langle u^2_{\rm app} \rangle = \langle u^2 \rangle_\omega = 0$ on instrumental resolution

The general form derived in Eq. (5) allows also a very intuitive understanding of the effect of different instrumental time resolution on the usually explored apparent MSD measured at $\omega = 0$ (see also Ref. [4, 14]):

$$\langle u^2_{\rm app} \rangle = \langle u^2 \rangle_{\omega=0} = -\lim_{q\to 0} \frac{3}{q^2} \log\left[S_{\rm exp}(q,0) \Big/ \hat{R}(0) \right] \qquad (9)$$

$$= \frac{3}{2\hat{R}(0)} \frac{1}{\sqrt{2\pi}} \int_{-\infty}^{\infty} dt\, \langle \Delta r^2 \rangle(t) R(t). \qquad (10)$$

Instead of measuring dynamical changes directly in the time or frequency domain as usually performed in quasi-elastic neutron scattering, the concept of the apparent MSD involves a different strategy: by fixing the time window with the instrumental resolution function $R(t)$, motions can

Table 1. Overview over generalized MSDs $\langle u^2\rangle_\omega$ arising from real MSDs $\langle \Delta r^2\rangle(t)$ and the energy transfer Ω^* at which $\langle u^2\rangle_\omega = 0$. For notational simplicity, we use dimensionless units: $\Omega = \omega/(\sqrt{2}\Delta\omega)$ and $\Lambda = \lambda/(\sqrt{2}\Delta\omega)$. The special functions are given by the so-called Dawson function $F_D(\Omega) = \exp(-\Omega^2)\int_0^\Omega dy\exp(y^2)$, the conventional Γ function $\Gamma(x)$, the so-called Kummer's confluent hypergeometric function $M[a,b,z]$ and $F_E(\Omega,\Lambda) = \frac{1}{2}\left(\exp[(\Lambda - i\Omega)^2][1-\mathrm{Erf}(\Lambda - i\Omega)] + \exp[(\Lambda + i\Omega)^2][1-\mathrm{Erf}(\Lambda + i\Omega)]\right)$ with the conventional error function $\mathrm{Erf}(x)$. The evaluations were performed using Mathematica.

Type of motion	Real MSD $\langle \Delta r^2\rangle(t)$	Generalized MSD $\langle u^2\rangle_\omega$	Energy of Zero $\langle u^2\rangle_\omega : \Omega^*$
Fast motions	σ^2	$\sigma^2\frac{3}{2\sqrt{2\pi}}$	∞
Free diffusion	$6D\lvert t\rvert$	$\frac{D}{\Delta\omega}\frac{9\exp(\Omega^2)}{\pi}[1-2\Omega F_D(\Omega)]$	0.924
Free ballistic motion	at^2	$\frac{a}{\Delta\omega^2}\frac{3(1-2\Omega^2)}{2\sqrt{2\pi}}$	$\sqrt{\frac{1}{2}} \approx 0.707$
Super- and sub-diffusive motions	$b^\alpha\lvert t\rvert^\alpha$	$\frac{b^\alpha}{\Delta\omega^\alpha}\frac{3\exp(\Omega^2)\,\Gamma\left[\frac{1+\alpha}{2}\right]M\left[\frac{1+\alpha}{2},\frac{1}{2},-\Omega^2\right]}{2^{(3-\alpha)/2}\pi}$	$0.331 + 0.983/\alpha - 0.541/\alpha^2 + 0.175/\alpha^3 - 0.023/\alpha^4$ (for $0.5 < \alpha < 2$)
Diffusion with confinement	$\sigma^2\left[1-\exp(-\lambda\lvert t\rvert)\right]$	$\sigma^2\frac{3}{2\sqrt{2\pi}}\left(1-\exp(\Omega^2)F_E(\Omega,\Lambda)\right)$	$0.924 + 0.0128\sqrt{\Lambda} + 0.2974\Lambda - 0.1222\sqrt{\Lambda}^3 + 0.02017\Lambda^2 - 0.00122\sqrt{\Lambda}^5$ (for $\Lambda < 30$)
Ballistic motion with confinement	$\sigma^2\left[1-\exp(-\lambda^2t^2)\right]$	$\frac{3\sigma^2}{2\sqrt{2\pi}}\left[1-\frac{1}{\sqrt{1+4\Lambda^2}}\exp\left(\frac{4\Lambda^2\Omega^2}{1+4\Lambda^2}\right)\right]$	$\frac{\sqrt{1+4\Lambda^2}\sqrt{\log[1+4\Lambda^2]}}{2\sqrt{2}\Lambda}$

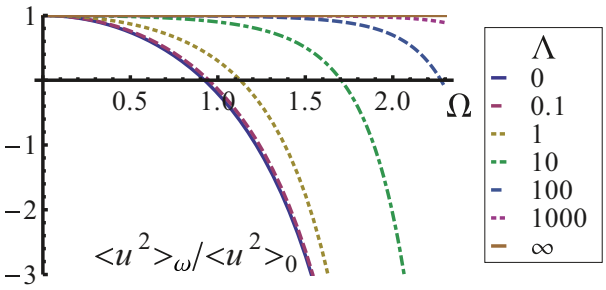

Figure 1. The generalized MSD $\langle u^2\rangle_\omega$ decays strongly with energy transfer $\Omega = \omega/(\Delta\omega\sqrt{2})$ for different relaxation constants $\Lambda = \lambda/(\Delta\omega\sqrt{2})$. $\Lambda = 0$ corresponds to the case of free diffusion. With increasing Λ, confinement effects become more and more prominent. Finally, $\Lambda = \infty$ represents the case of very fast short-time motions, in which case the motions have already explored the full space of confinement and only the confinement geometry is relevant on the measurement time scale. Similar behavior and trends are obtained for ballistic motions in confinement or subdiffusion with varying exponent α.

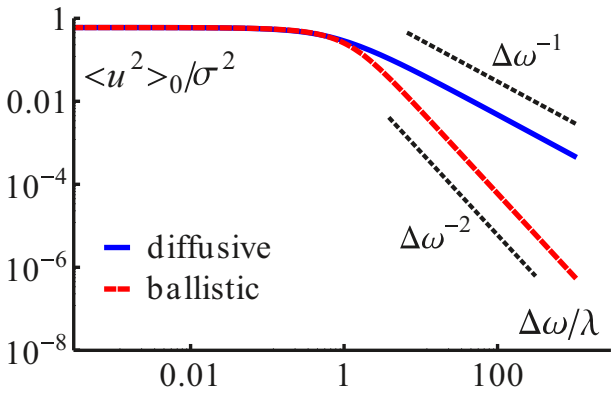

Figure 2. The apparent MSD $\langle u^2\rangle_0$ for the generic forms of diffusive and ballistic motions in confinement. For high resolutions, i.e. $\Delta\omega/\lambda \ll 1$, the dynamics explore the full confinement geometry characterized by σ^2 way before the instrumental time window. For more relaxed instrumental resolution, i.e. $\Delta\omega/\lambda \gg 1$, $\langle u^2\rangle_0$ scales as free diffusion and ballistic motion.

be explored only via spatial information, in particular using the positional correlation within a trajectory $\langle \Delta r^2\rangle(t)$. Figure 2 shows the MSD derived from the two generic models for diffusive and ballistic motion in confinement (see Table 1).

For high instrumental energy resolution compared to the motion, i.e. $\Delta\omega/\lambda \ll 1$, $\langle u^2\rangle_{\omega=0}$ is constant, evidencing that the dynamics have explored the full confinement way before the instrumental time window. The integral thus is simply an integration over the resolution function $R(t)$ with a constant prefactor σ^2. For more relaxed instrumental energy resolution, i.e. $\Delta\omega/\lambda \gg 1$, $\langle u^2\rangle_{\omega=0}$ scales as free diffusion and ballistic motion, respectively, evidencing that the dynamics are not affected by confinement inside the instrumental time window.

3. Energy of zero $\langle u^2\rangle_\omega$ as a model-free indicator of confinement effects

The generalized MSD $\langle u^2\rangle_\omega$ displays another interesting feature that can be used to extract information on the dynamics in a model-free manner. The energy Ω^*, at which $\langle u^2\rangle_{\Omega^*} = 0$, varies between the different models and parameters. Table 1 lists theoretical values and dependencies, and provides a series expansion for a reasonable parameter range if no closed analytic form has been derived. Depending on the value of Ω^* which can be reliably extracted via the change of sign in $\langle u^2\rangle_\omega$, the motion can be classified as described in the following paragraph.

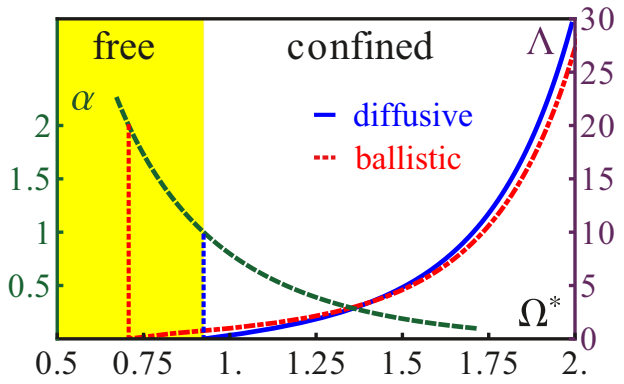

Figure 3. The dimensionless energy $\Omega^* = \omega^*/\Delta\omega/\sqrt{2}$ with $\langle u^2\rangle_{\Omega^*} = 0$ provides information on the effect of confinement on the dynamics on the instrumental time scale. For diffusive (solid) and ballistic (dash-dotted) motions in confinement, Ω^* increases with increasing $\Lambda = \lambda/\Delta\omega/\sqrt{2}$ (right axis) with the relaxation rate λ characterizing the onset of confinement. For $\Omega^* < 0.924$, only free super-diffusive motion with very weak confinement are present, whereas for $\Omega^* > 0.924$, sub-diffusive and confined motions indicate the presence of non-negligible obstacles or geometrical boundaries. Thus, $\langle u^2\rangle_{\omega^*}$ from a single inelastic fixed window scan at $\omega \approx \sqrt{2}\Delta\omega$ presents a model-free indicator on the presence of confinement within the sample in the instrumental time window.

In Fig. 3, the model parameters are depicted as a function of Ω^*. For low Ω^*, only super-diffusive motions with stretch exponent $\alpha > 2$, i.e. driven motions, are possible. At $\Omega^* = 1/\sqrt{2}$, free ballistic motion as a special case of super-diffusive motion sets in. In the regime $1/\sqrt{2} < \Omega^* < 0.924$, both free super-diffusive motions with $1 < \alpha < 2$ and ballistic motions with very weak confinement are possible. Above $\Omega^* > 0.924$, the effect of confinement on the instrumental time scale increases with increasing Ω^*. Alternatively, sub-diffusive motions could exist for these Ω^*, which imply that some kind of confinement or obstacles are present in the system.

The relations have been derived only for one motion on the instrumental time scale. In systems with hierarchical dynamics, Ω^* depends on all kinds of motions including the prefactors reflecting the amplitudes of the motions. It should be noted that the dominant motion for the determination of Ω^* in most cases corresponds to the slowest relevant diffusive motion on the instrumental time scale due to the steep decrease of $\langle u^2\rangle_\omega$ (Fig. 1).

Summarizing, $\langle u^2\rangle_\omega$ at $\omega \approx \sqrt{2}\Delta\omega$, i.e. $\Omega \approx 1$, allows a model-free monitoring whether confinement effects are important on the time scale of the instrument. For $\langle u^2\rangle_{\omega\approx\sqrt{2}\Delta\omega} > 0$, confinements effects are present, whereas $\langle u^2\rangle_{\omega\approx\sqrt{2}\Delta\omega} < 0$ indicates free or driven motions in the samples. While this property might not be so interesting for the case of full quasi-elastic spectra, it provides model-free information from an inelastic fixed window scan at only one energy. With more energies, the derived criterion on anomalous diffusion allows to monitor temporal changes of the strength of confinement e.g. due to temperature changes in their temporal development without explicit modeling.

4. Model-based analysis of elastic and inelastic fixed window scans

While we have so far explored model-free pathways of analysis, the full power of fixed window scans is found if the dependence of the scattering intensity from the elastic and inelastic fixed window scan on the parameter relevant to the system is complemented by a model for the dynamics, ideally validated from full quasi-elastic scans. Although it is in principle possible to calculate $\langle u^2\rangle_\omega$ for a given model in the spirit of Ref. [18], it is advisable to avoid the detour to dynamic information via the spatial information, since this procedure would face the same problems as discussed in Sect. 2.1. Instead, a direct fit of the intensity $S(q,\omega)$ from the model to the intensities of the elastic and inelastic fixed window scans proved powerful to yield a consistent picture of the evolution of dynamics [21,22,25]. With this approach using a combination of full quasi-elastic scans, elastic and inelastic fixed window scans, the evolution of $S_t(q,\omega)$ versus time or control parameter can be monitored on a grid of t and ω values that can be adapted to the specific system and phenomenon, thereby optimizing the usage and conclusiveness of experiments even during limited neutron beam time.

5. Conclusion

We have introduced the generalized mean-squared displacement (MSD) $\langle u^2\rangle_\omega$ as a model-free quantity obtainable from elastic and inelastic fixed-window scans. The dependence of $\langle u^2\rangle_\omega$ on instrumental resolution directly displays the general concept of the MSD analysis using spatial information from the q dependence in a fixed time window to indirectly extract information on the dynamics that are unaccessible in the instrumental time window.

$\langle u^2\rangle_\omega$ represents the Fourier transform of the real-time dependent MSD $\langle \Delta r^2\rangle(t)$ truncated by the instrumental time resolution. A direct back-transform is impossible due to the finite instrumental energy range and finite experimental errors. Nevertheless, the energy transfer ω^* at which $\langle u^2\rangle_{\omega^*} = 0$ can be used as a model-free indicator for the effect of confinement in the instrumental time window. While free motions correspond to $\omega^* < \sqrt{2}\Delta\omega$, a ω^* increasing beyond $\sqrt{2}\Delta\omega$ indicates increasing confinement. ω^* from $\langle u^2\rangle_\omega$ could be used as a first check on the dynamics, while the full power of elastic and inelastic fixed window scans is established in combination with models for the dynamics, ideally validated by full quasi-elastic spectra at few selected values within the parameter space of interest.

We profited from inspiring discussions with Marcus Hennig and Bernhard Frick (ILL, Grenoble) and are indebted to Marco Grimaldo (ILL, Grenoble) for constructive remarks on the manuscript.

References

[1] B. Frick, D. Richter, W. Petry, U. Buchenau, Z. Phys. B **70**, 73 (1988)
[2] J. Colmenero, A. Arbe, A. Alegria, Phys. Rev. Lett. **71**, 2603 (1993)
[3] R. Zorn, M. Mayorova, D. Richter, B. Frick, Soft Matter **4**, 522 (2008)
[4] S. Magazù, G. Maisano, F. Migliardo, C. Mondelli, Biophys. J. **86**, 3241 (2004)
[5] W. Doster, S. Cusack, W. Petry, Nature **337**, 754 (1989)
[6] F. Gabel, D. Bicout, U. Lehnert, M. Tehei, M. Weik, G. Zaccai, Q. Rev. Biophys. **35**, 327 (2002)
[7] J. Fitter, R. Lechner, N. Dencher, Biophys. J. **73**, 2126 (1997)
[8] P.W. Fenimore, H. Frauenfelder, B.H. McMahon, R.D. Young, Proc. Natl. Acad. Sci. USA **101**, 14408 (2004)
[9] K. Wood, M. Plazanet, F. Gabel, B. Kessler, D. Oesterhelt, D.J. Tobias, G. Zaccai, M. Weik, Proc. Natl. Acad. Sci. USA **104**, 18049 (2007)
[10] C. Mikl, J. Peters, M. Trapp, K. Kornmueller, W.J. Schneider, R. Prassl, J. Am. Chem. Soc. **133**, 13213 (2011)
[11] T. Becker, J.C. Smith, Phys. Rev. E **67**, 021904 (2003)
[12] S. Magazu, F. Migliardo, A. Benedetto, J. Phys. Chem. B **114**, 9268 (2010)
[13] G.R. Kneller, V. Calandrini, J. Chem. Phys. **126**, (2007)
[14] R. Zorn, Nucl. Instrum. Meth. A **603**, 439 (2009)
[15] G. Zaccai, J. Non-Cryst. Solids **357**, 615 (2011)
[16] D. Vural, H.R. Glyde, Phys. Rev. E **86**, 011926 (2012)
[17] M.T. Telling, S. Howells, J. Combet, L.A. Clifton, V. Garca Sakai, Chem. Phys. **424**, 32 (2013)
[18] M. Hennig, F. Roosen-Runge, F. Zhang, S. Zorn, M.W.A. Skoda, R.M.J. Jacobs, T. Seydel, F. Schreiber, Soft Matter **8**, 1628 (2012)
[19] F. Roosen-Runge, M. Hennig, F. Zhang, R.M.J. Jacobs, M. Sztucki, H. Schober, T. Seydel, F. Schreiber, Proc. Natl. Acad. Sci. USA **108**, 11815 (2011)
[20] B. Frick, J. Combet, L. van Eijck, Nucl. Instrum. Meth. A **669**, 7 (2012)
[21] M.T.F. Telling, L. Clifton, J. Combet, B. Frick, S. Howells, V. Garcia Sakai, Soft Matter **8**, 9529 (2012)
[22] A. Remhof, A. Züttel, T.A. Ramirez-Cuesta, V. Garca Sakai, B. Frick, Chem. Phys. **427**, 18 (2013)
[23] H.H. Grapengeter, B. Alefeld, R. Kosfeld, Colloid Polym. Sci. **265**, 226 (1987)
[24] D. Bicout, G. Zaccai, Biophys. J. **80**, 1115 (2001)
[25] M. Appel, B.Frick, et al.